

Electronic desorption of alkyl monolayers from silicon by very highly charged ions

T. Schenkel,^{a)} M. Schneider, M. Hattass, M. W. Newman, A. V. Barnes, A. V. Hamza, and D. H. Schneider

Lawrence Livermore National Laboratory, Livermore, California 94550

R. L. Cicero and C. E. D. Chidsey

Department of Chemistry, Stanford University, Stanford, California 94305

(Received 29 May 1998; accepted 16 September 1998)

Self-assembled alkyl monolayers on Si (111) were exposed to low doses of slow ($v \approx 6.6 \times 10^5$ m/s $\approx 0.3v_{\text{Bohr}}$), highly charged ions, like Xe⁴¹⁺ and Th⁷³⁺. Atomic force microscope images show craters from single ion impacts with diameters of 50–63 nm. Emission of secondary ions by highly charged projectiles was monitored by time-of-flight secondary ion mass spectrometry (TOF-SIMS). TOF-SIMS data give insights into the dependence of electronic desorption effects on the projectile charge state. We discuss the potential of highly charged projectiles as tools for materials modification on a nanometer scale. © 1998 American Vacuum Society.

[S0734-211X(98)13306-1]

I. INTRODUCTION

Recent advances in ion source technology have made slow (10^4 m/s $< v < 10^6$ m/s), very highly charged ions (HCI)—in principal up to U⁹²⁺—available for ion surface interaction studies.^{1–8} The characteristic features of the interaction of such highly charged ions with solids arise from their very rapid neutralization. Hundreds of keV of electronic excitation energy are deposited within 10 to 20 fs in a small target volume.^{2,6} Power densities are in the order of 10^{14} W/cm². Copious electron emission^{3,4} is followed by emission of high yields of secondary ions^{5,6} and neutrals.^{7–9} Sputter yields for metal oxides and semiconductors increase strongly as a function of projectile charge state or potential energy, respectively. For undoped GaAs (100), over 1000 atoms are ejected per Th⁷⁰⁺ projectile.⁸ Resulting from intense, ultrafast electronic excitation, sputter yields are largely independent of impact energy^{5,7} and primary ions can be used to modify surfaces at very low impact energies. Impact energies are limited by the image charge acceleration to ~ 1 keV (for U⁹⁰⁺ on carbon).¹⁰ The effect of highly charged ion impacts on materials topography was investigated first with mica targets where characteristic hillocks were observed after exposure to HCI.¹⁰ Atomic force microscope (AFM) images showed structures, ~ 0.5 nm high and with a base diameter of ~ 15 nm for Xe⁴⁴⁺ projectiles.^{11,12} Both high ablation rates and single ion induced topography changes mark promising effects for the development of novel materials modification techniques using slow, very highly charged ions (HCI). In this article we report on studies of the interaction of HCI with self-assembled alkyl monolayers (SAM) on Si(111).¹³ AFM images of SAMs after exposure to Xe⁴¹⁺ and Au⁶³⁺ show craters with diameters of 50–60 nm.

II. EXPERIMENT

Highly charged ions were extracted from the electron beam ion trap (EBIT) at Lawrence Livermore National Laboratory. The experimental setup for ion extraction and HCI based time-of-flight secondary ion mass spectrometry (TOF-SIMS) has previously been described.^{1–3,6} AFM images were obtained *ex situ* in noncontact, constant height mode with an Autoprobe LS (Park Scientific Instruments). AFM data were calibrated using a micron grating and previously measured hillock structures on mica. Self-assembled alkyl monolayers were deposited on Si(111).¹³ SAMs have been found to be stable in air over extended periods of time. CH₃(CH₂)₇, an untreated octene chain (SAM 1), and octene chains which had been chlorinated, sulfonamidated, and functionalized with CF₃-phenol (SAM 2), were exposed to Xe⁴¹⁺ and Au⁶³⁺ ions with velocities of $\sim 6.6 \times 10^5$ m/s ($0.3 v_{\text{Bohr}}$). Corresponding kinetic energies were 287 and 441 keV, respectively. Total ion doses were $\sim 10^9$ cm⁻², or ~ 10 μm^{-2} , low enough to void overlap of defects created by more than one HCI impact.

III. RESULTS AND DISCUSSION

A noncontact AFM image from the untreated octene SAM after exposure to Xe⁴¹⁺ is shown in Fig. 1. The average crater diameter is 51 ± 10 nm. The root mean square roughness of SAM 1 was 0.5 nm. Crater diameters on the functionalized SAM 2 after exposure to Au⁶³⁺ were at average 63 ± 14 nm. Typical noncontact tip radii were 70 nm and crater depths could not be determined with confidence from noncontact AFM data. The apparent crater depth was 3 nm, much larger than the thickness of the SAMs. The latter was ~ 0.8 nm for the octene chain and ~ 1.3 nm for SAM 2.¹³

^{a)}Electronic mail: SCHENKEL2@LLNL.GOV

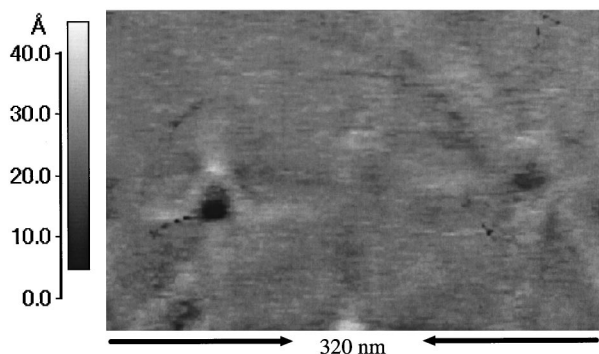


FIG. 1. Noncontact atomic force microscope image of an octene monolayer on Si (111) after exposure to Xe^{41+} . The average diameter of impact craters is 51 ± 10 nm.

We have monitored secondary ion emission from highly charged ion impacts by TOF-SIMS. Individual HCI trigger a start cycle by emission of electrons (for negatives) and protons^{5,6} (for positives). Sequentially arriving heavier secondary ions are detected as stops in a multistop timing analyzer. A highly charged ion based TOF-SIMS spectrum of negative secondary ions emitted from SAM 1 by Xe^{41+} ions is shown in Fig. 2. 10^6 ions impinged on the target for accumulation of the spectrum. Characteristic hydrocarbon chains reflect desorption and fragmentation of the octene chain in the impact event. The small peak at mass 28 u is likely to represent Si^- from the substrate. The number of negative molecular ions detected per Xe^{41+} impact is 0.08. The detection efficiency of the linear TOF-SIMS spectrometer with annular detector is ~ 0.1 – 0.15 . Ionization probabilities for positive and negative secondary ions emitted from SAMs under HCI bombardment are currently unknown.⁷ In Fig. 3 we show the region around mass 28 u in positive secondary ion spectra for three projectiles, Th^{73+} ($v = 5 \times 10^5$ m/s), Xe^{32+} ($v = 4.3 \times 10^5$ m/s) and Xe^{10+} ($v = 2.4 \times 10^5$ m/s). The target was a HC=CH-phenol SAM on Si (111) with a thickness of ~ 0.4 nm. Spectra for both Xe^{32+} and Th^{73+} are

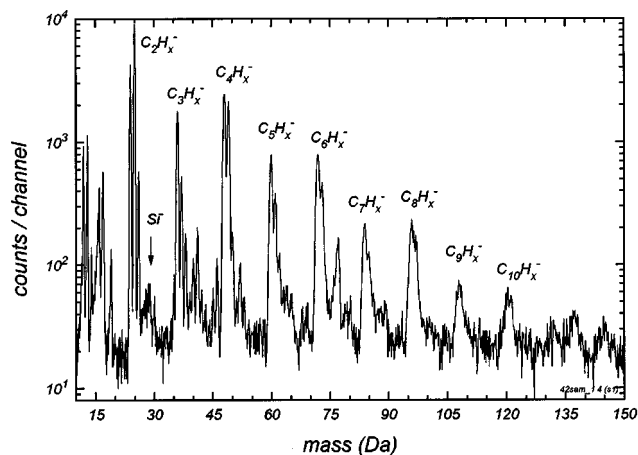


FIG. 2. Time-of-flight secondary ion mass spectrum of negative secondary ions from an octene monolayer on Si (111). Primary ions were Xe^{41+} with a kinetic energy of 410 keV.

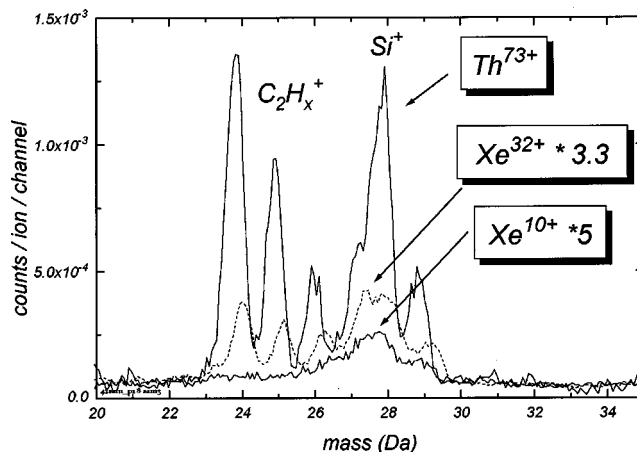


FIG. 3. Time-of-flight spectra of positive secondary ions desorbed from a HC=CH-phenol monolayer on Si (111) by Xe^{10+} , Xe^{32+} (dashed), and Th^{73+} projectiles.

dominated by C^+ . The mass resolution of the 10 cm long, linear TOF spectrometer was insufficient to resolve contributions from molecular ions CO^+ , C_2H_4^+ , etc. from the main silicon isotope. Future experiments will be conducted using a reflectron time-of-flight spectrometer. The lowest charge state ion, Xe^{10+} , emits only insignificant amounts of C^+ and C_2H_x^+ ions and the spectrum is dominated by mass 28 u ions. We interpret these as stemming from collisional sputtering of the silicon substrate. Increasing the projectile charge to Xe^{32+} and Th^{73+} , yields very strong increases of molecular ion yields from the SAM and of mass 28 u ions. The observation of craters following exposure to very highly charged ions is consistent with this observation of high yields of molecular ions and contributions from the silicon substrate. Our interpretation is that sufficiently highly charged ions damage and desorb material from the alkyl monolayers, forming the observed craters with areas of a few thousand square nanometers. The crater size gives a lower limit of the area damaged and chemically altered by individual highly charged ion impacts. For Xe^{41+} and SAM 1 the damage cross section is $\geq 2 \times 10^{-11}$ cm². Xe^{10+} does not carry enough electronic excitation energy to efficiently desorb the SAM directly, while the combined effect of kinetic energy loss and de-excitation damage the SAM in the impact area. In Fig. 4, we show the increase of positive secondary ion production from SAM 2 as a function of projectile charge state q . Projectiles were $\text{Xe}^{10+,32+,41+}$, Au^{69+} , and Th^{73+} with kinetic energies of 4 keV $\times q$. Positive secondary ion yields are largely independent of projectile velocity for velocities ranging from 10^5 to 10^6 m/s.^{5,7} AFM studies of a critical threshold excitation strength (i.e., projectile charge or potential energy) required for crater formation in SAMs are in progress.

IV. OUTLOOK

The direct removal of a layer of material from a silicon substrate over an area of a few thousand square nanometers could be employed as a direct write processing step in the fabrication of deep submicron devices. Having presented

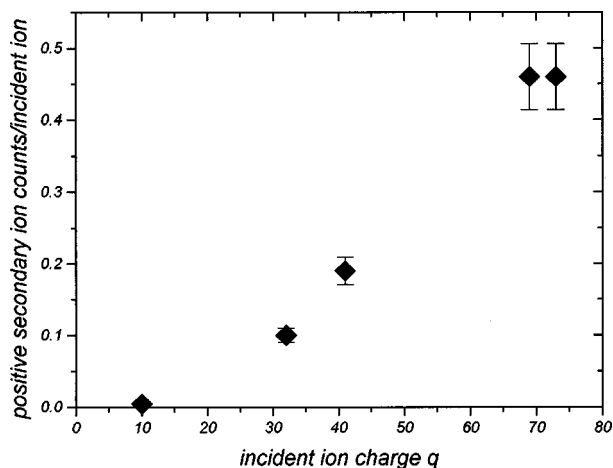


FIG. 4. Positive secondary ion production from a functionalized octene monolayer (SAM 2) on Si (111) as a function of projectile charge state q . The detection efficiency of the spectrometer is not included. Projectiles were $\text{Xe}^{10+,32+,41+}$, Au^{69+} , and Th^{73+} .

first evidence for this physical process we will now briefly discuss current availability of highly charged ions. Very highly charged ions, like Xe^{44+} and Th^{73+} can be extracted as low emittance ($\leq 1 \pi \text{ mm mrad}$)¹⁴ beams from electron beam ion traps (EBIT).¹ EBITs are compact ($\sim 1 \text{ m}$ in length), relatively inexpensive devices. Delivery of a Xe^{44+} flux in the order of 10^6 – 10^7 ions/s is routinely achieved.^{3,15} Future source development should allow to push this limit by at least a factor of 10. The random exposure of a 1 cm^2 sample area requires at present a time in the order of ~ 15 min for an impact density of $50 \text{ Xe}^{44+}/\mu\text{m}^2$. Focusing of HCI beams to a spot with $20 \mu\text{m}$ diameter has been demonstrated.¹⁴ Spot sizes $< 100 \text{ nm}$, common for liquid metal ion guns, are currently not available for HCI. Very recent model calculations suggest the possibility for optimization of beam brightness, i.e., the number of ions extracted per unit solid angle and area per second, by over two orders of magnitude by employing ion cooling techniques during extraction.¹⁴ An alternative to beam focusing could be the steering of arrays of HCI. Here, HCI are retrapped and cooled in a Penning trap¹⁶ where they can undergo a phase transition to a crystalline state (“Coulomb crystals”). This HCI condensate can then be dumped onto a surface, where the crystal pattern is imprinted.

In order for HCI based materials modification techniques to develop and mature, the characterization of fundamental physical processes in HCI solid interactions will have to be accompanied by ambitious development of high brightness HCI sources.

V. SUMMARY

Self-assembled alkyl monolayers on Si (111) were exposed to slow, very highly charged ions. Noncontact AFM images show craters from single ion impacts. Crater diameters are $51 \pm 10 \text{ nm}$ for Xe^{41+} impact on octene chains on Si (111). Highly charged ion based secondary ion mass spectrometry gives additional evidence for the efficient removal of alkyl layers from the silicon substrate by electronic desorption. We discuss the current availability of highly charged ions as tools for deep submicron processing.

ACKNOWLEDGMENT

This work was performed under the auspices of the U.S. Dept. of Energy by Lawrence Livermore National Laboratory under Contract No. W-7405-ENG-48.

- ¹R. E. Marrs, P. Beiersdorfer, and D. Schneider, *Phys. Today* **47**, 27 (1994); D. Schneider, M. W. Clark, B. M. Penetrante, J. McDonald, D. DeWitt, and J. N. Bardsley, *Phys. Rev. A* **44**, 3119 (1991).
- ²T. Schenkel, M. A. Briere, A. V. Barnes, A. V. Hamza, H. Schmidt-Böcking, K. Bethge, and D. H. Schneider, *Phys. Rev. Lett.* **78**, 2481 (1997); **79**, 2030 (1997); T. Schenkel, A. V. Hamza, A. V. Barnes, and D. H. Schneider, *Phys. Rev. A* **56**, R1701 (1997).
- ³D. H. Schneider and M. A. Briere, *Phys. Scr.* **53**, 228 (1996).
- ⁴J. W. McDonald, D. Schneider, M. W. Clark, and D. Dewitt, *Phys. Rev. Lett.* **68**, 2297 (1992).
- ⁵T. Schenkel, A. V. Barnes, M. A. Briere, A. V. Hamza, A. Schach von Wittenau, and D. Schneider, *Nucl. Instrum. Methods Phys. Res. B* **125**, 153 (1997).
- ⁶T. Schenkel, M. A. Briere, H. Schmidt-Böcking, K. Bethge, and D. Schneider, *Mater. Sci. Forum* **248/249**, 413 (1997); T. Schenkel, A. V. Hamza, A. V. Barnes, D. S. Walsh, B. L. Doyle, and D. Schneider, *J. Vac. Sci. Technol. A* **16**, 1384 (1998).
- ⁷T. Schenkel, A. V. Barnes, A. V. Hamza, D. Schneider, J. C. Banks, and B. L. Doyle, *Phys. Rev. Lett.* **80**, 4325 (1998).
- ⁸T. Schenkel, A. V. Barnes, A. V. Hamza, D. Schneider, J. C. Banks, and B. L. Doyle, *Phys. Rev. Lett.* **81**, 2590 (1998).
- ⁹M. Sporn, G. Libiseller, T. Neidhard, M. Schmid, F. Aumayr, H. P. Winter, P. Varga, M. Grether, D. Niemann, and N. Stolterfoht, *Phys. Rev. Lett.* **79**, 945 (1997).
- ¹⁰F. Aumayr, H. Kurz, D. Schneider, M. A. Briere, J. W. McDonald, C. E. Cunningham, and H. P. Winter, *Phys. Rev. Lett.* **71**, 1943 (1993).
- ¹¹D. Schneider, M. A. Briere, M. W. Clark, J. McDonald, J. Biersack, and W. Siekhaus, *Surf. Sci.* **294**, 403 (1993); C. Ruehlicke, M. A. Briere, and D. Schneider, *Nucl. Instrum. Methods Phys. Res. B* **99**, 528 (1995).
- ¹²D. C. Parks, M. P. Stockli, E. W. Bell, L. P. Ratkliff, R. W. Schmieder, F. G. Serpa, and J. D. Gillaspay, *Nucl. Instrum. Methods Phys. Res. B* **134**, 46 (1998).
- ¹³M. R. Linford, P. Fenter, P. M. Eisenberg, and C. E. D. Chidsey, *J. Am. Chem. Soc.* **117**, 3145 (1995).
- ¹⁴R. E. Marrs, D. H. Schneider, and J. W. McDonald, *Rev. Sci. Instrum.* **69**, 204 (1998); R. E. Marrs (unpublished).
- ¹⁵L. P. Ratkliff, E. W. Bell, D. C. Parks, A. I. Pikin, and J. D. Gillaspay, *Rev. Sci. Instrum.* **68**, 1998 (1997).
- ¹⁶D. Schneider, D. A. Church, G. Weinberg, J. Steiger, B. Beck, J. McDonald, E. Magee, and D. Knapp, *Rev. Sci. Instrum.* **65**, 3472 (1994).